ARTICLE

Corona Discharge Ion Mobility Spectrometry of Ten Alcohols†

Hai-yan Han[a], Hong-mei Wang[a], Hai-he Jiang[a], Michal Stano[b], Martin Sabo[b], Stefan Matejcik[b], Yan-nan Chu[a*]

a. Laboratory of Environmental Spectroscopy, Anhui Institute of Optics and Fine Mechanics, Chinese Academy of Sciences, Hefei 230031, China
b. Department of Experimental Physics, Comenius University, Bratislava 84248, Slovak Republic

(Dated: Received on August 5, 2009; Accepted on November 17, 2009)

Ion mobility spectra for ten alcohols have been studied in an ion mobility spectrometry apparatus equipped with a corona discharge ionization source. Using protonated water cluster ions as the reactant ions and clean air as the drift gas, the alcohols exhibit different product ion characteristic peaks in their ion mobility spectra. The detection limit for these alcohols is at low concentration pmol/L level according to the concentration calibration by exponential dilution method. Based on the measured ion mobilities, several chemical physics parameters of the ion-molecular interaction at atmosphere were obtained, including the ionic collision cross sections, diffusion coefficients, collision rate constants, and the ionic radii under the hard-sphere model approximation.

Key words: Reduced mobility, Hard-sphere model, Ion molecular collision parameters

I. INTRODUCTION

Since ion mobility spectrometry (IMS) was first introduced in the early 1970s [1], it has been developed as a trace analytical technique [2,3] based on the fact that ions have different drift velocities at ambient pressure as they move in a low electric field. The main advantages of IMS instruments are their high sensitivity, small size, and operation at atmospheric pressure, which makes that IMS have been widely applied in many fields, such as narcotics and explosives detection [4,5], environment pollution monitoring [6,7], disease diagnosis [8,9], structure analysis of clusters [10,11] and biomolecules [12,13].

The capability of IMS to detect alcohols was demonstrated by several research groups [14−17]. In these measurements, the ionization sources employed in the IMS were radioactive ^{63}Ni material. Although the ^{63}Ni ionization source has some benefits such as its stability, simplicity, and no need extra power supply, there exist some shortages in terms of regular leak test and waste disposal. In addition, the ion generation rate of ^{63}Ni source is not high enough and result in a limited sensitivity and dynamic measurement range. In 2001, Sielemann *et al.* reported the detection of alcohols using the non-radioactive UV photo-ionization ion mobility spectrometry (UV-IMS) equipped with a 10.6 eV lamp [18]. The available detection limitation was about a few μmol/L.

Recently, another non-radioactive ionization source, discharge ionization source has been combined with IMS [19−21]. Some researches have found that the ion current obtained from the corona ionization source is larger than that of the ^{63}Ni ionization source, which can lead to a higher signal-to-noise ratio and better sensitivity [20]. For instance, a limit of detection at low pmol/L level for six alcohols has been achieved in our previous corona discharge IMS (CD-IMS) experiments [22].

Most studies of IMS with different ionization sources focus on the mobility spectra, reduced motilities, and limit of detection. However, IMS technique can be used to investigate the interactions between the ions and neutral molecules in the drift tube. In this work, ten alcoholic compounds have been systematically restudied in a corona discharge ion mobility spectrometer. Besides the mobility spectra, the reduced mobilities, and the detection limitations, some important chemical physics parameters concerning ionic interactions are derived from the spectral measurements based on a hard sphere model approximation, including collision cross sections, diffusion coefficients, ionic radii, and collision rate constants.

II. EXPERIMENTS

The corona discharge ion mobility spectrometer constructed in our laboratory is schematically shown in Fig.1. It mainly consists of the ionization source, ion-molecule reaction region, drift region, and detection system. The corona discharge ionization source has a point-to-plane geometry, and a typical discharge voltage

†Part of the special issue for "the Chinese Chemical Society's 11th National Chemical Dynamics Symposium".
*Author to whom correspondence should be addressed. E-mail: ychu@aiofm.ac.cn, FAX: +86-551-5591076

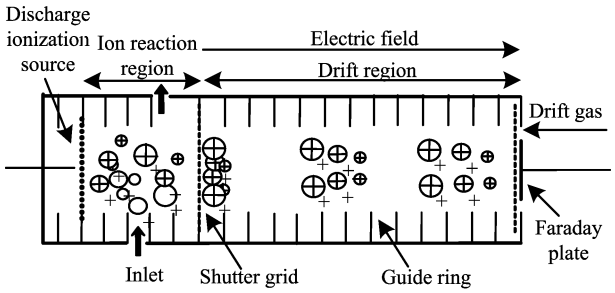

FIG. 1 Schematic diagram of ion mobility spectrometry apparatus.

on the corona needle is around 3 kV. The drift tube has a full length of 17 cm with internal diameter of 4 cm. The guide rings of the drift tube are electronically insulated from each other by 1 mm thick Teflon spacer, and a high voltage is distributed through a series of resistors on these rings so that a uniform electric field along the axis of drift tube is formed. The electric field strength in both reaction and drift region can be adjustable in the range of 250−400 V/cm. The analyte is injected to the reaction region by a carrier gas flow. The drift gas is introduced into the drift tube from the end of drift tube in order to wash the internal wall of drift tube and to keep the drift region clean. There is a shutter grid between the reaction region and the drift region, which consists of two series of parallel wires biased to a potential to create an orthogonal field relative to the drift field and can be switched periodically to inject the pulses of ions into the downstream drift tube. The ionic pulse width can vary from 100 μs to 300 μs. In the drift region, the ions will be separated according to their ion mobilities, which depend on the mass and structure of the ions. The ion current is collected by a faraday plate and an amplified signal is fed to the computer data processing system. The ion current versus the drift time is recorded as the ion mobility spectrum.

The temperature and pressure in the drift tube are kept at 298 K and 101 kPa, respectively. The drift and carrier gases used in these experiments are purified air, filtered with the 13X molecular sieves. The flow rates were 300 and 500 mL/min for the carrier gas and drift gas, respectively. All of the chemical reagents are analytical reagents with the purities of above 99.7%.

III. RESULTS AND DISCUSSION

A. Theory

The ions are separated in the drift region according to their masses and structures. The average velocity of the ions in the gas is called drift velocity, which is directly proportional to the electric field intensity in the drift region by following equation [23].

$$v = KE \tag{1}$$

where v is the velocity of ions, the proportionality coefficient K is the ion mobility, and E is the electrostatic field. If ionic drift length is L, transit time in drift region is t, the ionic mobility can be derived according to the equation,

$$K = \frac{v}{E} = \frac{L}{Et} \tag{2}$$

The ion mobility is usually normalized to the reduced mobility K_0 at standard conditions (273 K and 101 kPa) as it is shown in Eq.(3), which makes the experimental values comparable under different pressure and temperature conditions.

$$K_0 = \frac{P}{760}\frac{273}{T}K \tag{3}$$

Theoretically, the ion mobility K depends on ionic mass, collision cross section, and the number density of the drift gas is shown in Eq.(4).

$$K = \frac{v}{E} = \frac{3\sqrt{2\pi}}{16}\frac{q}{N}\sqrt{\frac{1}{\mu k_{\mathrm{B}}T}}\frac{1+\alpha}{\Omega} \tag{4}$$

In Eq.(4), q is the ionic charge, N is the number density of the neutral drift gas, μ is reduced mass which can be expressed by $mM/(m+M)$, m and M are the masses of the ion and the neutral molecule respectively, k_{B} is the Boltzmann constant, T is the temperature, α is a small correction term with a magnitude of less than 0.02, when the ion mass is larger than the mass of the drift gas molecule, and Ω is the average ion molecular collision cross section. From the Eq.(4) it can be seen that IMS can be used to separate isomers of a compound, because of the different collision cross sections and therefore different ion mobilities. The differences in collision cross section can arise from differences in either geometrical structure or the internal charge distribution, or both.

The collision cross section is defined as the average collision integral between the ion and a neutral drift gas [23]. Several methods have been employed to estimate collision cross sections from molecular modeling calculations [24] such as exact hard spheres model [25], the trajectory and the scattering on electron density method. In this work, we discuss the collision cross section values of the alcohol ions with the molecules of the drift gas mainly using the hard spheres model [26].

Under the assumptions of the hard sphere model, the collision cross section is reduced to Eq.(5),

$$\Omega = \pi\left(r_{\mathrm{ion}} + r_{\mathrm{gas}}\right)^2 \tag{5}$$

where r_{ion} is the ion radius and r_{gas} is the neural molecular radius of the drift gas. When we assume that the

DOI:10.1088/1674-0068/22/06/605-610

ions are nearly spherical, the radius of the ions are calculated by using the following equation,

$$r_{\rm ion} = \sqrt{\frac{\Omega}{\pi}} - r_{\rm gas} \tag{6}$$

Based on the hard spheres model, we may apply the crudest method to calculate the collision rate constant $k_{\rm HS}$ between ions and the neural molecules, where the energy dependence of the cross sections is neglected.

$$k_{\rm HS} = \sqrt{\frac{8\pi k_{\rm B}T}{\mu}} d^2 \tag{7}$$

where μ is the reduced mass just as described in Eq.(4), d is the sum of the hard sphere radii of the ions and the neural molecules ($r_{\rm ion}$+$r_{\rm gas}$).

According to the Einstein relation, the mobility at low electric field strengths is related to the diffusion coefficient, D, which describes the diffusion of the ions in the drift gas. The relation is known in following form:

$$K_0 = \frac{qD}{k_{\rm B}T} \tag{8}$$

This relation proves to be useful in relating ion mobility spectrometry results to analogous data on the diffusion of charged ions through air. According to this equation, the diffusion coefficient of ions in the drift gas can be easily obtained, which offers a simple method to measure this parameter in chemical physics research.

B. Reactant ion peak

The reactant ions are produced continuously in corona discharge ion source and are extracted by the electric field and introduced into the reaction region. In the absence of sample molecules, the reactant ions pass through the reaction region practically without any chemical reactions and exhibit a distinct spectrum governed by experimental parameters of pressure, temperature, electric field, moisture, and drift length. Figure 2 presents the spectrum measured without introduction of any sample gas, in which only one reactant ion peak (RIP) is observable. According to Eq.(2) and Eq.(3), the reduced mobility of this peak is 2.17 $\rm cm^2/(V{\cdot}s)$, which is very close to the reported mobility values of $(H_2O)_3H^+$ and $(H_2O)_4H^+$ (2.26 and 2.19 $\rm cm^2/(V{\cdot}s)$) [27]. Therefore, the reactant ions formed in the ion source mainly include $(H_2O)_nH^+$ (n=3, 4). Increase in temperature causes the RIP to change in position, this is due to the declustering of the hydrated cluster ions as reported by Eiceman and co-workers [28], who studied the ion mobility spectral variation of the protonated water cluster ions $(H_2O)_nH^+$ with temperature and moisture of the drifting air. In clean air, the hydrated protons $(H_2O)_nH^+$ are the dominant ions which are produced through a series of ion-molecule reactions

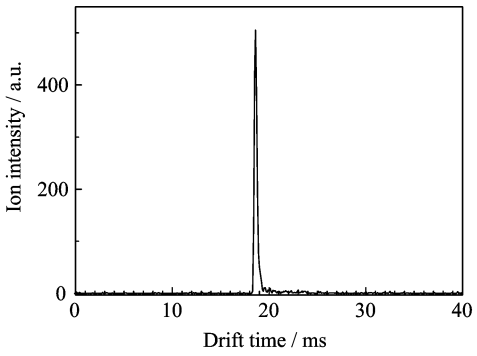

FIG. 2 High resolution ion mobility spectrum of RIP.

initiated by ionization of N_2 and H_2O in the corona discharge and subsequent conversion of the primary discharge ions in collision with water present in the IMS. The reaction ions formation has been introduced previously [22].

C. Mobility spectra and detection limitation

When sample molecules (M) are injected into the reaction region, the reactant ions undergo collisions with them. If the cluster ions $(H_2O)_nH^+$ are used as reagent ions, the ion-molecule reaction between the reactant ion and the sample molecule can proceeds only when the proton affinity (PA) of the sample molecule is greater than that of water or water cluster, producing possible molecular product ions as follows [29]

$$(H_2O)_nH^+ + M \rightarrow (H_2O)_{n-1}MH^+ + H_2O \tag{9}$$

The proton affinities of the samples can be obtained at NIST Chemistry WebBook (http://webbook.nist.gov/chemistry). It is known that the PA of alcohol is always higher than that of the water. Thus the alcohols studied in this work can be formed in the reaction region of IMS via the proton transfer reactions between the reactant ions and alcohol molecules. The rate of the reactions is established by the collision frequency, the concentration of the reactant ions $(H_2O)_nH^+$, and the concentration of the sample molecules.

In the experiments, when the alcohol sample is injected to the reaction region of the ion mobility spectrometer with a concentration of pmol/L in the clean air carrier gas, the intensity of the reactant ions immediately declined and new ion peak appeared in the longer drift time domain. The mobility spectra of ten alcohol samples are illustrated in Fig.3. The reduced mobility values of the samples are at the right of the ion peak in Fig.3. It can be found that, the ionic drift time increases with the increasing ion mass, thus the ion mobility decreases with ion mass according to Eq.(4).

In order to investigate the sensitivity of the ion mobility spectrometer, the exponential dilution flask (EDF)

DOI:10.1088/1674-0068/22/06/605-610

TABLE I Several chemical physics parameters of ten alcohol samples determined by CD-IMS with air as drift gas.

Compound	M/a.u.	$K_0/(\mathrm{cm}^2/(\mathrm{Vs}))$	$\Omega/\mathrm{Å}^2$	$r_{\mathrm{ion}}/\mathrm{Å}$	$k_{\mathrm{HS}}/(10^{-10}\mathrm{cm}^3/\mathrm{s})$	$D/(10^{-2}\mathrm{cm}^2/\mathrm{s})$
Ethanol	46	2.06	123	4.52	3.87	5.35
2-propanol	60	1.98	125	4.57	3.76	5.04
Propanol	60	1.92	128	4.63	3.87	4.93
2-methyl-2-propanol	74	1.90	125	4.57	3.64	4.88
2-butanol	74	1.88	126	4.60	3.70	4.83
2-methyl-1-propanol	74	1.85	128	4.65	3.78	4.75
Butanol	74	1.82	130	4.70	3.87	4.68
Isoamyl alcohol	88	1.74	133	4.78	3.90	4.47
Amyl alcohol	88	1.72	135	4.81	3.96	4.42
2-octanol	130	1.51	148	5.11	4.29	3.88

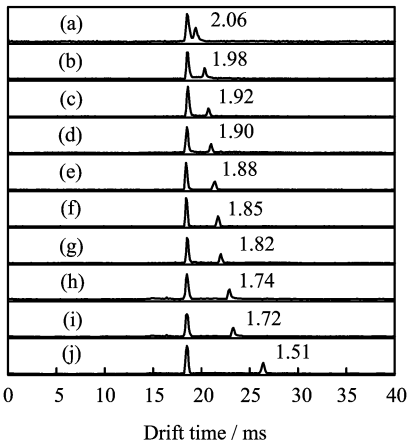

FIG. 3 Ion mobility spectra of ten alcohols measured in the CD-IMS. The labeled numbers beside the product ion peaks are the reduced mobilities. (a) Ethanol, (b) 2-propanol, (c) Propanol, (d) 2-methyl-2-propanol, (e) 2-butanol, (f) 2-methyl-1-propanol, (g) butanol, (h) isoamyl alcohol, (i) amyl alcohol, and (j) 2-octanol.

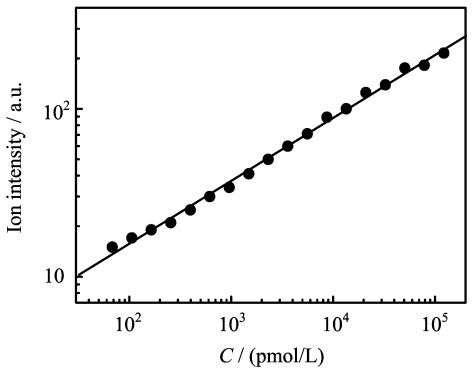

FIG. 4 Dependence of ion intensity on butanol concentration.

[30] is used to generate the different concentrations of the samples. The concentration C of a sample gas varies with the dilution time,

$$C = C_0 \exp\left(-\frac{Qt}{V}\right) \tag{10}$$

where C_0 is the initial concentration in the EDF, Q is the flow rate of the carrier gas, t is the dilution time and V is the volume of the dilution flask. A magnetic stirrer is used to make the vapor mixture homogenous. The alcohol vapors in the flask were injected into the reaction region of IMS by the carrier gas through a Teflon tube connected with the flask. The volume of the glass flask was 680 mL, and flow rate of the carrier gas was around 300 mL/min.

When the samples were injected into the reaction region of the ion mobility spectrometer at a high concentration beyond several ppm, the protonated dimer ions $(H_2O)_mM_2H^+$ appeared in the spectrum, which were formed due to the ion-molecule reactions between the protonated monomer ions $(H_2O)_mMH^+$ and the neutral alcohol molecules. This is seen in a mobility spectrum as a further decrease in the peak intensity of the reactant ion, a decrease in peak height of the protonated monomer, and an appearance of a third peak at a drift time longer than that for the protonated monomer. As the concentration of the sample was reduced, the intensity of the monomer ions was increasing and the dimer ions $(H_2O)_mM_2H^+$ was decreasing till disappearance. If the sample concentration diminished further, the peak height of the monomer ions $(H_2O)_mMH^+$ started to gradually decrease, finally approaching to the detection limit level. As an example, Figure 4 shows the ionic intensity dependence on alcoholic concentration, from which a detection limit at several pmol/L was obtained for the detection of butanol.

D. Reduced mobilities and Ion collisions parameters

The K_0 values for ten alcohols, determined according to the Eq.(4), are listed in Table I. The reduced mobility values decrease with the increasing in the ions masses of alcohols, which indicates the drift time of ion in the IMS is primarily proportional to the mass of the

DOI:10.1088/1674-0068/22/06/605-610

product ions. The accuracy of the K_0 measurement was in present experiment 5%.

The Ω related to the size and shape of the molecule was obtained using Eq.(4) when the gas density (pressure), temperature, and charge number was constant (Table I). From the results, we can see that, as the mass of the sample molecules is increasing, the collision cross section is increasing. For the isomer ions the collision cross sections are different due to the different geometrical structure of the ions. For example, the cross section of the four butanol isomers 2-methyl-2-propanol, 2-butanol, 2-methyl-1-propanol, and butanol are different each from other. The discrimination between isomeric compounds is difficult to perform by MS alone but has been shown to easily achieve with high-resolution IMS instruments. The influence of the structure on ion mobility has been reported earlier [31]. The general rules for the dependence of the ion mobility on the ionic structure are applicable to these alcohols in following order: linear<branched, primary<secondary<tertiary.

According to Eq.(4) we can see that the reciprocal mobility $(1/K)$ is proportional to the product of the collision cross section and the reciprocal square root of the reduced mass $\mu^{-1/2}$. For the alcohol samples with increasing chain length of the alkyl chain, a plot of the reciprocal reduced mobility against square root of the reduced mass should give an upward bent curve reflecting the increasing collision cross section with the increasing mass. This expected behavior is clearly seen from Fig.5, which indicates, that the drift time of ion in the IMS is primarily proportional to the mass of the product ions [32].

The radius of the ion strongly affects the distance of approach to the neutral gas molecule, and correspondingly, the interaction parameters. In the hard-sphere model, it means that the sum of the radium of the ion and the neutral molecule, d, will increase slightly as the chain length and ion mass in the homologous series increase. After substitution of the Ω into Eq.(4), the radii of the ions were obtained which are shown in Table I, in Eq.(6) the $r_{\rm gas}$ was approximated by the air molecular effective radius of 1.75 Å. The reduced mobility of propanol (1.92 $cm^2/(V{\cdot}s)$) is larger than the mobility of 2-methyl-2-propanol (1.90 $cm^2/(V{\cdot}s)$), but the radius is smaller than that of 2-methyl-2-propanol, this indicates that for small mass molecule (not much larger than the drift gas molecule) the mass affects more the reduced ion mobility than the structure of the ion. Under the assumptions of hard-sphere model, the ions determined in this work were considered to be nearly spherical, which brings a little deviation between the measurement values and the true values. The rate constants calculated with Eq.(7) are in the range of 3.64×10^{-10} cm^3/s for 2-methyl-2-propanol to 4.29×10^{-10} cm^3/s for ethanol.

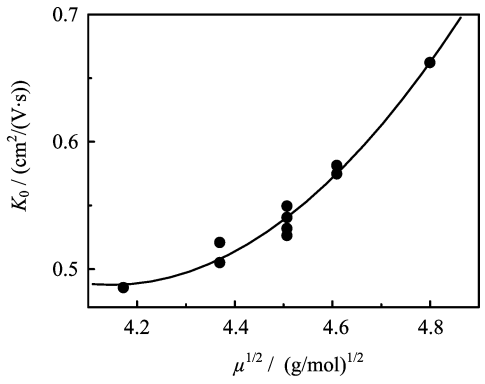

FIG. 5 Dependence of reduced mobility on ionic mass.

D, the protonated ions formed from sample molecules in the clean air, calculated according to Eq.(8) are found to be in the range from 3.88×10^{-2} cm^2/s for 2-octanol to 5.35×10^{-2} cm^2/s for ethanol. The diffusion coefficients values are listed in Table I.

IV. CONCLUSION

The reactant ions, hydrated cluster ions, are generated in the IMS apparatus using a corona discharge ionization source. Using the proton transfer ionization of the selected alcohols and the IMS technique, the reduced mobilities of the alcohols were determined. The ionization reactions in the CD-IMS appeared to be similar to the ion chemical processes in the traditional Ni-IMS. The exponential dilution experiment showed that the detection limit of the CD-IMS is in the order of magnitude of several ppb. Using the hard-sphere model, several chemical physics parameters for the ion-molecular collision were obtained including the collision cross section, diffusion coefficients, collision rate constants, and the ionic radii of the alcohol molecules.

V. ACKNOWLEDGMENTS

This work was support by the National Natural Science Foundation of China (No.20577049, No.20707025, and No.20907054), the Chinese-Slovak Scientific and Technological Cooperation Project (No.4-03), the Excellent Youth Foundation of Anhui Province Scientific Committee (No.06045098), the Hefei Institutes of Physical Science, Chinese Academy of Science are gratefully acknowledged, and the Slovak Research and Development Agency, projects (No.LPP-0143-06 and No.SK-CN-029-07).

[1] M. J. Cohen and F. W. Karasek, J. Chromatogr. Sci. **8**, 330 (1970).
[2] R. H. Stlouis and H. H. Hill, Crit. Rev. Anal. Chem. **21**, 321 (1990).
[3] G. A. Eiceman, Crit. Rev. Anal. Chem. **22**, 17 (1991).

DOI:10.1088/1674-0068/22/06/605-610

[4] R. G. Ewing, D. A. Atkinson, G. A. Eiceman, and G. J. Ewing, Talanta **54**, 515 (2001).
[5] C. Wu, W. E. Steiner, P. S. Tornatore, L. M. Matz, W. F. Siems, D. A. Atkinson, and H. H. Hill, Talanta **57**, 123 (2002).
[6] A. B. Kanu, H. H. Hill, M. M. Gribb, and R. N. Walters, J. Environ. Monitor. **9**, 51 (2007).
[7] C. J. Koester, A. Moulik, Anal. Chem. **77**, 3737 (2005).
[8] V. Ruzsanyi, J. I. Baumbach, S. Sielemann, P. Litterst, M. Westhoff, and L. Freitag, J. Chromatogr. A **1084**, 145 (2005).
[9] Z. Karpas, B. Tilman, R. Gdalevsky, and A. Lorber, Anal. Chim. Acta **463**, 155 (2002).
[10] E. Oger, R. Kelting, P. Weis, A. Lechtken, D. Schooss, N. R. M. Crawford, R. Ahlrichs, and M. M. Kappes, J. Chem. Phys. **130**, 124305 (2009).
[11] P. Weis, Int. J. Mass Spectrom. **245**, 1 (2005).
[12] D. E. Clemmer and M. F. Jarrold, J. Mass Spectrom. **32**, 577 (1997).
[13] G. A. Eiceman, D. B. Shoff, C. S. Harden, A. P. Snyder, P. M. Martinez, M. E. Fleischer, and M. L. Watkins, Anal. Chem. **61**, 1093 (1989).
[14] Z. Karpas, Struct. Chem. **3**, 139 (1992).
[15] A. J. Bell, K. Giles, S. Moody, N. J. Underwood, and P. Watts, Int. J. Mass Spectrom. **165**, 169 (1997).
[16] D. M. Myton and R. J. Obrien, Anal. Chem. **63**, 1201 (1991).
[17] A. J. Bell, K. Giles, S. Moody, and P. Watts, Int. J. Mass Spectrom. **173**, 65 (1998).
[18] S. Sielemann, J. I. Baumbach, H. Schmidt, and P. Pilzecker, Anal. Chim. Acta **431**, 293 (2001).
[19] H. Borsdorf, H. Schelhorn, J. Flachowsky, H. R. Doring, and J. Stach, Anal. Chim. Acta. **403**, 235 (2000).
[20] M. Tabrizchi, T. Khayamian, and N. Taj, Rev. Sci. Instrum. **71**, 2321 (2000).
[21] S. K. Ross and A. J. Bell, Int. J. Mass Spectrom. **218**, L1 (2002).
[22] H. Y. Han, G. D. Huang, S. P. Jin, P. C. Zheng, G. H. Xu, J. Q. Li, H. M. Wang, and Y. N. Chu, J. Environ Sci. Chin. **19**, 751 (2007).
[23] H. E. Revercomb and E. A. Mason, Anal. Chem. **47**, 970 (1975).
[24] T. Wyttenbach, G. VonHelden, and M. T. Bowers, J. Am. Chem. Soc. **118**, 8355 (1996).
[25] A. A. Shvartsburg and M. F. Jarrold, Chem. Phys. Lett. **261**, 86 (1996).
[26] C. Illenseer and H. G. Lohmannsroben, Phys. Chem. Chem. Phys. **3**, 2388 (2001).
[27] S. H. Kim, K. R. Betty, and F. W. Karasek, Anal. Chem. **50**, 2006 (1978).
[28] D. Young, C. L. P. Thomas, J. Breach, A. H. Brittain, and G. A. Eiceman, Anal. Chim. Acta **381**, 69 (1999).
[29] R. G. Ewing, G. A. Eiceman, and J. A. Stone, Int. J. Mass Spectrom. **193**, 57 (1999).
[30] J. J. Ritter and N. K. Adams, Anal. Chem. **48**, 612 (1976).
[31] Z. Karpas, Anal. Chem. **61**, 684 (1989).
[32] Z. Berant and Z. Karpas, J. Am. Chem. Soc. **111**, 3819 (1989).

DOI:10.1088/1674-0068/22/06/605-610